Laser Interferometry Determination on Thermal Effects of Diode-End-Pumped Nd: YVO_4 Laser

Peng Xiaoyuan[a], Anand Asundi[a], Chen Yihong[b], Xiong Zhengjun[b], G. C. Lim[b]

[a]Sensors and Actuators Program, Nanyang Technological University, Nanyang Avenue, Singapore 639798

[b]Gintic Institute of Manufacturing Technology, 71 Nanyang Drive, Singapore 638075

ABSTRACT

Thermal effects of diode-end-pumped solid state laser operating on lasing and non-lasing states are discussed in this paper. It is found that thermal effects under lasing operation are quite different from those of non-lasing operation. Thermal effects have been measured quantitatively under actual lasing conditions using laser interferometry. The proposed technique is set up to determine the optical path difference (OPD) resulting from thermal effects in crystal with high resolution. More importantly, it provides noninvasive measurement means with high sensitivity which circumvents the limitation of conventional techniques. The measurement results of thermal effects offer a crucial basis to optimize the design of laser resonator with high-power end-pumped geometry.

Keywords : Thermal Effects, Laser Interferometer, Diode-End-Pumping, Solid State Laser

I. INTRODUCTION

Recently, neodymium-doped yttrium orthovanadate (Nd: YVO4) crystal has been considered as promising lasing material for diode-pumped lasers. For an example, a diode end-pumped Nd: YVO4 laser with up to 35 W of average power in a polarized TEM_{00} mode has been demonstrated by Spectra-Physics Lasers.[1] Thereafter, it is possible to scale the output power of vanadate laser host materials to higher level. Nd: YVO4 crystal has many advantages including high gain cross section, low threshold, and wide absorption bandwidth. However, thermal effects, which result from physical deformation, temperature-induced and stress-induced changes in the refractive index of gain medium, dramatically influence the stability, output power and beam quality because Nd: YVO4 has higher thermal absorption and lower thermal conductivity coefficient than other laser materials such as Nd: YAG. Therefore, average output power of Nd: YVO4 lasers is much lower than that of diode pumped Nd: YAG lasers.[2] As a large amount of thermal energy converted from absorbed pump power is accumulated near the pump region in end geometry, the maximum laser output power of Nd: YVO4 is limited by thermal effects. The oscillating mode of a laser resonator with an active lens is changed with thermal lensing effect, which influences the stability of resonator and slope efficiency of lasing operation.[3] However, in a practical laser system, thermal effects of lasing crystal depend on material properties, cooling scheme, and pump source. Theoretical analysis can only predict a trend of thermal effects versus pump power. Therefore, it is noted that quantitative determination of thermal effects will contribute significantly to correctly design a cavity with a mode that matches the pump volume to achieve good laser efficiency and good beam quality.

Various techniques to measure the induced thermal lens have been reported, which were not only employed in flashlamp-pumped solid state laser, but also developed in the area of diode-pumped solid state laser. Typically, the measurement of thermal effects can be classified into two methods: non-interferometry and interferometry. In

conventional non-interferometry, a collimated probe beam is incident into a laser crystal considered as a lens-like medium, and the focused probe beam is recorded by a CCD camera.[4] Pinhole test [5] and " knife-edge"[6] test are the two typical non-interferometric methods. Such simple technique has sufficient temporal resolution, but suffers from poor spatial resolution where the pumping region is very small part of cross section of the lasing crystal. Thus, this kind of non-interferometric method is inappropriate in end-pumped systems. Unlike interferometric method, it can not detect an absolute phase change. Conventional interferometers such as Michelson and Mach-Zehnder interferometers have been designed to achieve high spatial resolution.[7-8] Unfortunately, these reported interferometers are difficult to operate under actual lasing condition, since additional optical elements are needed in the laser system. This will change the condition of laser operation, and influence the pump loading and lasing output. Recently, Blows[9-10] developed a holographic lateral shearing interferometry to measure the thermal effects with lasing action. However, a polarizing beam-splitter (PBS) cube was still needed placed inside the resonator which will increase the intracavity losses, and in turn influence the quantitative measurement of thermal effects.

Thermal effects of end-pumped crystal under lasing condition are quite different from non-lasing condition, which will be comparatively investigated in the next part. The pertinent result shows that temperature distributions in the crystal without lasing action are correspondingly higher than those with lasing action. Since the design basis of resonator depends on thermal lensing measured, it is crucial to measure thermal effects under actual lasing condition.[11]

In this paper, a laser interferometer, which provides a non-invasive, full field, high-resolution and real-time means for diagnosing thermal effects by measuring optical path difference (OPD) induced by thermal loading in Nd: YVO_4 crystal, is presented. Different from traditional measurement approaches, it can be operated on the actual working condition. The thermal beam distortions in the Nd: YVO4 crystal are measured with a He-Ne laser at the wavelength 632.8nm. The deformation of the rod with increasing pump power is encoded in the changes of interference patterns. The experimental results of effective thermal lens power versus pump power are obtained, and the optimal design of laser cavity taking into account thermal effects can be achieved.

II. MEASUREMENTS

2.1. Thermal effects under lasing / non-lasing condition

In thermal analysis, a parameter, called fractional thermal load (ξ), is defined as the fraction of absorbed input power contributing to heating of the crystal. Measurements of ξ for different lasing materials have been made by researchers.[12-14] ξ parameter of Nd: YAG crystal was measured in the range from 0.29 [12] to 0.53 [13]. The values were quite different, in which the reason partly can be explained by the measurement errors on one hand, and on the other hand mainly caused by the different measurement conditions with and without lasing actions. The variance of thermal effects under lasing and non-lasing conditions is studied in this paper by measuring the temperature distribution in the crystal.

In order to compare the temperature distribution in the lasing crystal under different working conditions, an infrared thermometer (IT2 – 50 and IT 2–02) provided by Keyence corp. is employed to measure temperature at end pumping face. The infrared radiation thermometer offers convenient applications of measuring surface temperature of coated and optical pumped crystal in a non-contact way with high sensitivity. Relevant parameters of the infrared thermometer are as follows: resolution up to 0.1 °C, accuracy of ±1% of F. S., and response time of 0.5 s.

The values of temperature at different points of the end-pumping face are measured by adjusting the indicative beam of the thermometer sensor to the interest positions. Since the minimum measurement size of the sensor is ϕ 1.2 mm, the testing temperature is the average over this size. The setup for measuring temperature of end-pumped crystal is shown in Figure. 1. A conventional stable plano-concave resonator is configured between a high

reflective flat mirror, which is the end face of laser crystal, and 89% reflective concave output coupler with a curvature radius of 800mm. The laser medium, Nd: YVO_4 rod, fabricated by Casix Company, is $3 \times 3 \times 5$ mm with Nd doping of 0.5 %. It has a 1.06 μm AR coating at one end, 1.06 μm HR coating and 808 nm AR coating at the other end. The rod is end-pumped by a 15 W fiber-coupled diode laser with numerical aperture of 0.16 and diameter of 1.5 mm (OPC - A015- mm– FC) from Opto Power Corporation. The fiber output is focused to a spot of 600μm by a collimating and focusing optics. The length of the cavity is 100 mm which results in a mode waist diameter of 600 μm at the flat mirror. The shutter in the cavity is used to control the working conditions of resonator in lasing and non-lasing actions. Two kinds of cooling scheme are used in our experiments: first, the crystal laterally wrapped in indium foil layer is mounted by two water-cooled copper blocks from top and bottom for heat removal. Second, the crystal mounted in the copper blocks without water-cooling operates at room temperature.

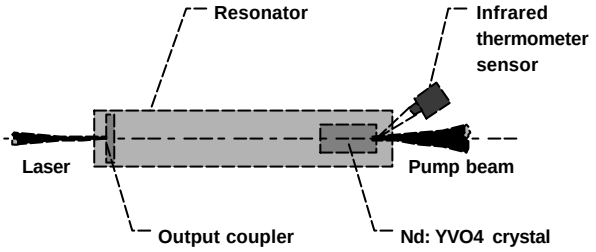

Figure 1 Schematic setup of temperature measurement using infrared thermometer

Figure 2 (a) and (b) shows the temperature distributions of lasing and non-lasing actions at the pumping end face of the crystal under different cooling conditions and pump power. The pump power of 6.4 W and 4.6 W correspondingly excites the output power of 3.2 W and 2.4 W with the resonator design mentioned above.

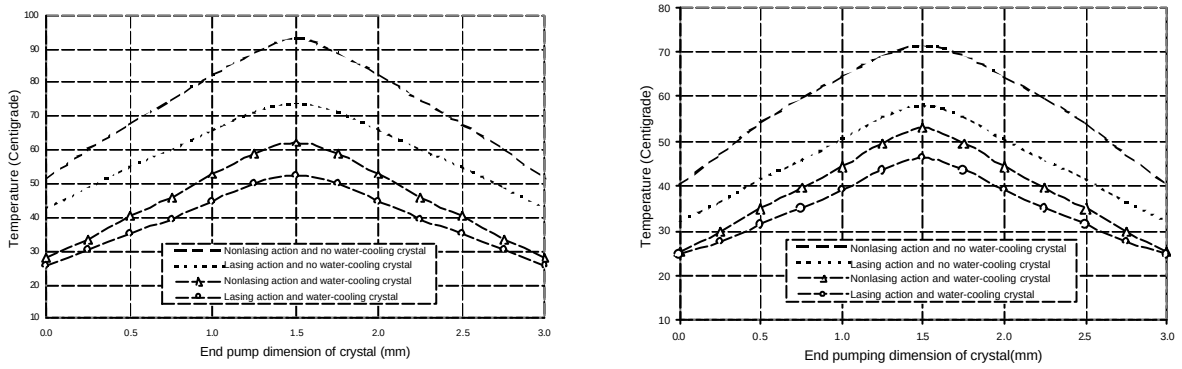

(a) (b)

Figure 2 Temperature distributions in the lasing crystal with lasing and non-lasing action

Figure 2(a) is with the pump power of 6.4 W in lasing and non-lasing conditions. The crystal operates in two cooling states: water-cooling with temperature of 23 °C and room temperature. Figure 2(b) is with the pump power of 4.6 W and non-lasing conditions. The crystal operates in two cooling states: water-cooling with temperature of 23 °C and room temperature.

The gradient for temperature distributions from the central part of the pumping end face to the peripheral of the crystal represents thermal effects induced by heat deposition in lasing crystal. On the one hand, the temperature-

dependent variation of refractive index will be raised with the increase of temperature gradient. On the other hand, the stress distribution will become larger corresponding to the higher gradient in the crystal, which in turn physically elongates the crystal in the longitudinal direction. The curves in Figure 2 exhibit thermal effects by the temperature distribution under lasing and non-lasing conditions. In addition, the comparison is extended to the crystal under different cooling conditions. Based on the measurement results of temperature distributions at the end fact of the crystal, we may summary as follows:

- The temperature gradients from the central part to the edge of the crystal under non-lasing conditions are much larger than those under lasing conditions with the same pump power and cooling state.
- In a certain pump power, the temperature gradients from the central part to the edge of the crystal under non-lasing conditions are higher than those under lasing conditions regardless of the cooling states.
- The temperature gradients are correspondingly larger when the pump power is increased.
- In our experimental conditions, the temperature gradients under non-lasing condition increase about 20% - 25% compared with lasing conditions.

In our experiments, when the optical-to-optical efficiency is relatively lower induced by the misalignment of resonator, the temperature gradient will be increased. Therefore, note that thermal effects in the actual working condition will be quite different from those in the non-lasing condition. With the aim of designing a practical laser resonator under the conditions of high-power pumping, the quantitative measurement of thermal effects without any influence on actual lasing operation becomes very important.

A quantitative measurement is carried out in the setup shown in Figure 3 to determine the thermal lensing effect by measuring the OPD in lasing medium. The thermal lensing effect is calculated by interferometric measurement of the thermal-induced OPD changes under lasing condition.

.

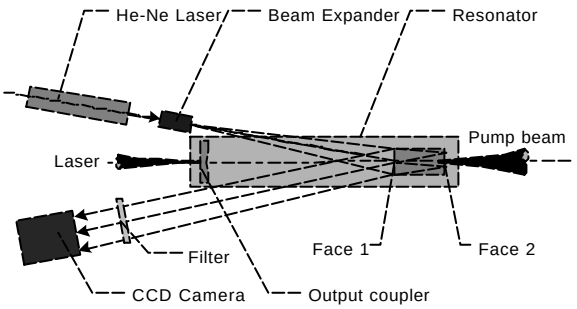

Figure 3. Schematic layout of the laser interferometer used to measure thermal effects

A frequency stabilized He-Ne laser is employed as an interferometric probe beam with a wavelength of 632.8nm. The thermal beam distortions in a Nd:YVO_4 rod are quantitatively measured from interferograms. The interference occurs between the wave fronts reflected from the front (F) and the back (B) surface of the crystal, shown in Figure 1. The generated interference patterns are imaged with a CCD camera connected to a PC for calculation and analysis. The total optical path difference (OPD) induced by the changes in both of refractive index and physical length L of the crystal can be expressed as

$$OPD = n\Delta L + L\Delta n, \tag{1}$$

where Δn and ΔL are the changes in refractive index and physical length, respectively. A series of consecutive interferograms are captured with increasing pump power to record the progressive variation process in a Nd:YVO_4 crystal induced by accumulated thermal lensing effects. These are six typical fringe patterns taken from the series

of interferograms, which are shown in Figure 2 (a)-(f). Figure 2 (a) corresponds to the initial state of lasing crystal with no pump source, other five interferograms are with Gaussian beam loading under lasing condition with the pump power of 2.5 W, 3.5 W, 5.4 W, 6.4 W and 8.3 W respectively. It should be mentioned that the crystal operates at the room temperature.

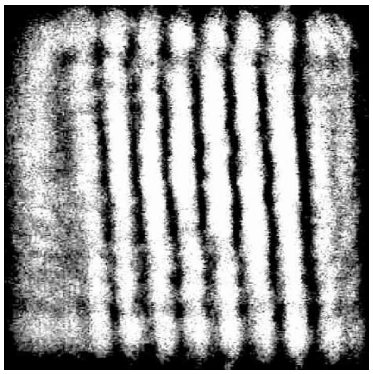

(a) Without diode pumping, served as the reference pattern

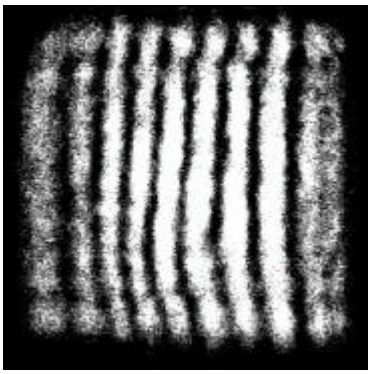

(b*) Pumping power: 2.5 Watts ($2w_p' = 600mm$)*

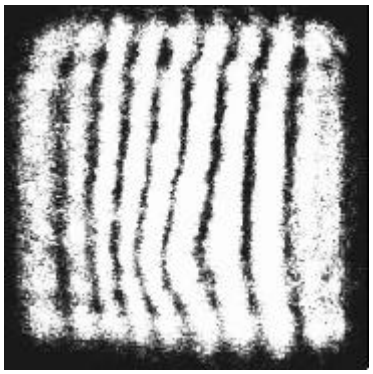

(c) Pumping power: 3.5 Watts ($2w_p' = 600mm$)

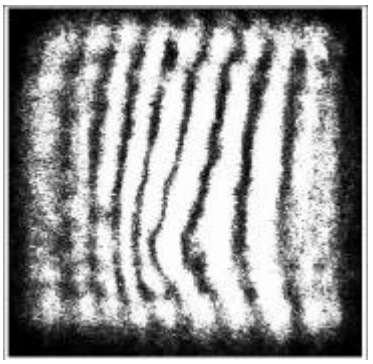

(c) Pumping power: 5.4 Watts ($2w_p' = 600mm$)

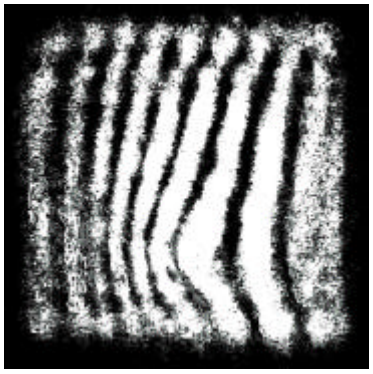

(e) Pumping power: 6.4 Watts ($2w_p' = 600mm$)

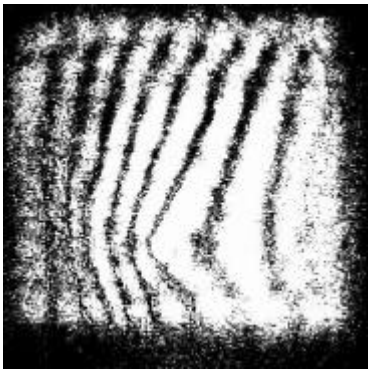

(f) Pumping power: 8.3 Watts ($2w_p' = 600mm$)

Figure 4. Interferograms of an end-pumped Nd:YVO_4 rod with a probing wavelength of $\lambda = 632.8nm$

In Figure 4, ω_p' is the diameter of pump beam at the end face of the crystal. It is observed that besides the continuous unitary shift of the fringes, the interference patterns at the pump area exhibits more serious distortions

with the increase of pump power. It can be explained that the temperature gradients in the rod are increased with diode beam loading, and thermal effects mainly occur at the pump region. In addition, the shift in the number of fringe patterns, except the pump region, shows linear trend with pump power, which can be explained the entire temperature of the crystal is raised with the pump power. The degree of the variation of fringes records the change of Optical Path Difference in the crystal induced by the thermal effects. Thus the effective focal length of the lasing crystal can be calculated.

III. RESULTS AND DISCUSSION

Laser interferometric based measurement system is successfully employed in monitoring thermal effects in Nd:YVO_4 crystal under actual lasing conditions. The measured temperature distribution at pumping end face and distortions of fringe patterns for Nd: YVO_4 crystal display severe thermal effects. The measured values of thermal lensing power as a function of the absorbed pump power in the Nd: YVO_4 crystal are shown in Figure 5.

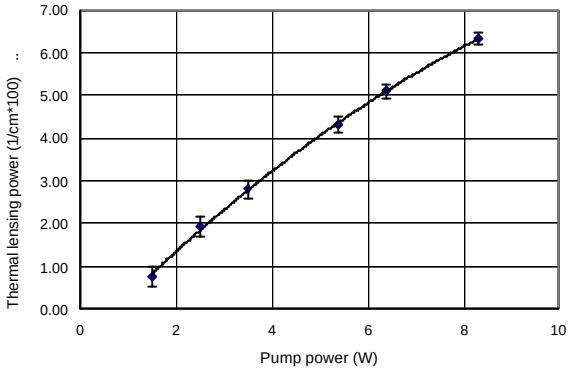

Figure 5. Thermal lensing power vs. pump power

Data shown in Figure 5 demonstrate that the thermal lensing power becomes serious with the increment of pump power. The variation range of focal length is from 1320 mm to 158 mm with the pump power increasing from 1.34 W to 8.3 W. It is quite possible that the stability of the resonator will be affected under such a wide variation of the active focusing lens. It is a crucial essential to design a laser resonator.

There are two factors accounting for thermal lensing effect in a diode-pumped laser medium: thermal part (the change of the refractive index due to temperature gradient, the change of the refractive index due to thermal stress), and end effect (the change of the physical length due to thermal expansion). The temperature-dependent variation of the refractive index constitutes the major contribution of the thermal lens[7]. The changes of OPD obtained from the laser interferometry record both the thermal part and end effect in the crystal. The temperature distributions and temperature gradients at the pumping end face reveal end effect and a part of change of temperature-dependent variation of refractive index.

We may compare the change of temperature gradients with the measurement thermal lensing power under different absorbed pump power. The temperature gradients increase 22% when the absorbed pump power changes from 4.6 W to 6.4 W, while the thermal lensing power raises 32%. It indicates that thermal effects under non-lasing condition compared with lasing conditions will be more serious than the value of 20% - 25% we obtained in last section. In addition, the major thermal effects are generated in the range of pump region and end face because of the larger absorption coefficient of Nd: YVO_4 crystal.

The data contained in Figure 5 can be directly used to design a cavity which accommodates the severe thermal effects with end-pumping geometry.

By checking the theoretical prediction, it is so surprised that thermal lensing power of Nd: YVO_4 is much smaller than measurement result, which was also observed in Nd: YAG crystal by Hodgson[2] recently.

The change of refractive index can be written as[7]

$$n(r) = n_0[1-\frac{Q}{2K}(\frac{1}{2n_0}\frac{dn}{dT}+n_0{}^2aC_{r,f})r^2], \tag{2}$$

where C_r, and C_ϕ are functions of the elastooptical coefficients of Nd:YVO_4, K is the thermal conductivity of Nd:YVO_4, Q is the heat source function (heat generated per unit volume), n_0 is the refractive index, dn/dT is the thermal index, α is the absorption coefficient, and r is the radius variation of the rod.

The theoretical focal length of an end-pumping structure is given by[7]

$$f_{th} = \frac{KA}{P_A}(\frac{1}{2}\frac{dn}{dT}+aC_{r,f}n_0{}^3+\frac{ar_0r_0(n_0-1)}{L_r})^{-1}, \tag{3}$$

where A is the rod cross-sectional area, P_A is the total heat dissipated in the rod, r_0 is the radius of the rod, and L_r is the length of rod.

Ignoring the end effect and stress-induced variation of refractive index, Eq. (3) can be simplified as

$$f_{th} = \frac{KA}{P_p(\frac{dn}{dT})}(\frac{1}{1-e^{-aL_r}}), \tag{4}$$

where K = 0.051 W cm^{-1} K^{-1}, α = 12.4cm^{-1} (0.5% Nd doping), P_p is the absorbed pump power, L_r = 0.5cm, and dn/dT = 8.5× 10^{-6} /k.

Figure 6 gives the relationship curve of thermal lensing power vs. absorbed pump power obtained theoretically which is the solid line. For comparison, the measured curve is also shown in this figure.

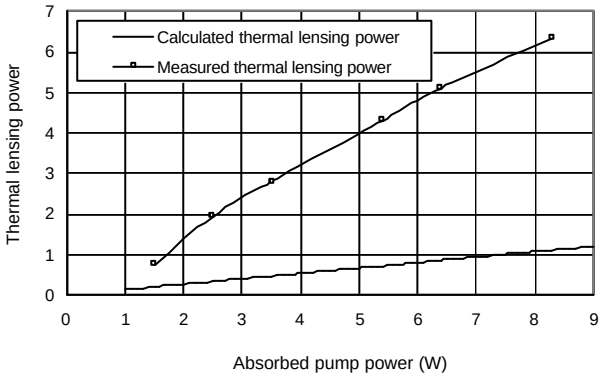

Figure 6 Thermal lensing power vs. absorbed pump power

It is found from Figure 6 that the measured thermal lensing power is much larger than the theoretical result. This kind of considerable deviation between these two results cannot be adequately explained by the fact that only the

thermally induced variation of refractive index is considered in Eq. (4), while measured results are affected by all the three temperature-dependent effects. Currently, it has been supposed to be the reason of upconversion which should be further studied theoretically.

IV. CONCLUSIONS

A simple and efficient infrared thermometer is applied to directly test the temperature distribution at the end-pumping face of the crystal. The differences of temperature distributions and temperature gradients in lasing and non-lasing conditions are observed. It can be confirmed that thermal effects under non-lasing condition compared with lasing conditions will be larger than the value of 20% - 25%.

A laser interferometer is employed with high resolution and sensitivity to measure the change of OPD in laser crystal under lasing condition. It provides noninvasive, real time and full field measurement. The experimental and theoretical results of thermal lensing power versus pump power are obtained, and the large deviations between the two results are indicated. Based on the measured thermal lensing power, together with the theory of active resonator, the optimal resonator circumventing the severe thermal effects can be designed in high-power end-pumping geometry.

ACKNOWLEDGEMENTS

The authors would like to thank NSTB, Gintic, NTU and MPE supporting the project through the grant No. I99-P0-129, in-house project No. C98-P-142A, and MLC1/97 respectively. Keyence Corporation providing the infrared thermometer is also acknowledged.

REFERENCE

1. Paula M. Noaker, and John Wallace, "CLEO'99 tackles the science and technology of light", *Laser Focus world*, 35 (5), 127 – 134 (1999).

2. N. Hodgson, K. D. Griswold, W. A. Jordan, S. L. Knapp, A. A. Peirce, C. C Pohalski, E. A. Cheng, J. Cole, D. R Dudley, A. B. Petersen, W. L. Nighan (1999), High power TEM_{00} mode operation of diode-pumped solid-state lasers, *SPIE proceedings*, vol.3611, 119-131(1999).

3. S. C. Tidwell, J. F. Seamans, M. S. Bowers, and A. K. Cousins, Scaling CW diode-end-pumped Nd:YAG lasers to high average powers, *IEEE Journal of Quantum Electronics*, 28 (4), 997-1009 (1992).

4. D. S. Sumida, D. A. Rockwell, and M. S. Mangir, Energy storage and heating measurements in flashlamp-pumped Cr: Nd: GSGG and Nd: YAG, *IEEE Journal of Quantum Electronics*, 24 (6), pp. 985-994, 1988.

5. W. K. Lee, and C. C. Davis, " Laser interferometric studies of laser-induced surface heating and deformation" ,*IEEE J. of Quantum Electronics*, 22 (4), pp. 569-573, 1986.

6. C. S. Zhen, and Q. Q. Hu, Thermal effects of diode-pumped anisotropic gain mediums, *Chinese J. of Lasers*, 24 (8), pp. 659-684, 1997.

7. W. Koechner, *Solid-state laser engineering (Third Edition)*, Spronger-Verlag, USA, pp. 388-392, 1992.

8. J. M. Laurenzano, B. W. Liby, K. H. Greives, and J. O. Grannis, Analysis of thermal effects in crystalline media using a dual-interferometer, OSA TOPS on Advanced Solid-state Lasers, Vol. I, pp. 227-230, 1996.

9. J. L. Blows, T. Omatsu, J. Dawes, H. Pask, and M. Tateda, Heat genteration in Nd: YVO_4 with and without action, *IEEE Photonics Technology Letters*, 10 (12), pp. 1727-1729, 1998.

10. J. L. Blows, J. Dawes, and T. Omatsu, Thermal lensing measurements in line-focus end-pumped neodymium yttrium aluminum garnet using holographic lateral shearing interferometry, *Journal of Applied Physics*, 83 (6), pp. 2901-2906, 1998.

11. A. Asundi, X. Y. Peng, Y. H. Chen, Z. J. Xiong, G. C. Lim, H. Y. Zheng, Thermal effects of diode end-pumped Nd:YVO_4 solid state laser, *SPIE proceedings*, Vol. 3898, pp. 178-185, 1999.

12. T. Y. Fan, Heat generation in Nd YAG and Yb: YAG, *IEEE Journal of Quantum Electronics*, 29 (6), pp. 1457-1459, 1993.

13. T. S. Chen, V. L. Anderson, and O. Kahan, Measurements of heating and energy storage in diode-pumped Nd: YAG, *IEEE Journal of Quantum Electronics*, 26 (1), pp. 6-8, 1990.

14. C. Pfistner, R. Weber, H. P. Weber, S. Merazzi, and R. Gruber (1994), Thermal beam distortions in end-pumped Nd: YAG, Nd: GSGG, and N:YLF rods, *IEEE J. of Quantum Electronics*, 30 (7), pp. 1605-1615.